Journal of Mining and Environment (JME), Vol. 15, No. 2, 2024, 597-611

Shahrood University of Technology

Journal of Mining and Environment (JME)

Journal homepage: www.jme.shahroodut.ac.ir

Iranian Society of Mining Engineering (IRSME)

Delineation of Gold Exploration Targets based on Prospectivity Models through an Optimization Algorithm

Kamran Mostafaei[1]*, Mohammadnabi Kianpour[2], and Mahyar Yousefi[3]

1. Department of Mining, Faculty of Engineering, University of Kurdistan, Sanandaj, Iran, Corresponding author
2. Faculty of Mining Engineering, Amirkabir University of Technology, Tehran, Iran
3. Faculty of Engineering, Malayer University, Malayer, Iran

Article Info

Received 13 August 2023

Received in Revised form 24 September 2023

Accepted 30 September 2023

Published online 30 September 2023

DOI: 10.22044/jme.2023.13472.2489

Keywords

Mineral prospectivity mapping

Gray Wolf Optimizer algorithm

Gold exploration targets

Abstract

Mineral prospectivity mapping (MPM) is a multi-staged process aiming at delimiting exploration targets. Experts' knowledge is an indispensable component of MPM, and might be required (i) while translating signature features of ore-forming processes into a suite of maps, namely evidence layers, (ii) while assigning weights to evidence layers, and (iii) while interpreting maps of mineral prospectivity. The latter is important as MPM integrates weighted evidence layers into a continuous map of mineral prospectivity. Although high values in prospectivity maps pertain to prospective zones, maps of mineral prospectivity are devoid of interpretation. One, therefore, should adopt a classification scheme to categorize or prioritize exploration targets from a map of mineral prospectivity. In addition to previous frameworks applied for interpreting maps of mineral prospectivity, this paper introduces an optimization-based framework, the Gray Wolf Optimizer (GWO) algorithm, for addressing this problem. In addition to GWO, we also used percentile maps of 85, 90, and 95% for interpreting the results of our prospectivity model. These methods were applied to a fuzzy-based map of mineral prospectivity derived for the Alut area, NW Iran. Overall, the map derived by the GWO has involved more Au occurrences, 66% of explored Au occurrences by GWO versus 33% by percentile maps; also introduces more targets as high-potential zones of Au mineralization that may be neglected by traditional methods like percentile maps.

1. Introduction

Given the dwindling number of successful exploration projects, controlling the ever-rising risk and cost of exploration surveys appears important. Mineral prospectivity mapping (MPM) helps to modulate the risk of exploration surveys by reducing the search spaces. Geological knowledge linked to mathematical computational techniques is the base for MPM [1-5]. The knowledge of ore-forming processes helps the translation of critical processes involved in the formation of mineral deposits into a set of suite predictor variables, i.e. a series of maps deemed exploration targeting criteria [6-11]. The exploration values in the maps are then weighted and combined through mathematical and statistical frameworks for generating predictive maps of mineral prospectivity [12-15].

MPM aims to reduce the search radius in green field regions but they still need to be optimized to reduce the required time and cost of exploratory efforts. Swarm intelligence algorithms could be considered ideal for reaching this purpose [16-20].

The swarm intelligence algorithms including the Gray Wolf Optimizer (GWO) algorithm have an origin in the strategies that living beings use to fulfill their needs like hunting, nesting, etc. Such algorithms are being applied to solve complicated problems by providing rapid and rational solutions [21, 22]. Swarm intelligence algorithm possesses high-value properties consisting of self-organization, parallel, distributive, flexibility, and robustness, so has given special importance to these algorithms in various domains of science including electronic power systems,

Corresponding author: K.mostafaei@uok.ac.ir (K. Mostafaei)

communication networks, system identification, parameter estimation, robot control, transportation, and other practical engineering issues [22-25].

Accordingly, the investigation of the swarm intelligence optimization algorithms leads to precious output and results. The GWO has been widely used in problem-solving of various subjects including solving optimal reactive power dispatch problems [26], inversion of geoelectrical data [27], optimization, and solving engineering design problems [28].

Many studies have been centered on optimizing fuzzy-logic-based prospectivity models by improving the effectiveness index [29-34]. However, these studies have not used algorithm optimization tools. Therefore, this study seeks to answer whether using model optimization algorithms can improve the effectiveness index of fuzzy-logic-based prospectivity models. This paper intends to bridge this knowledge gap by applying a metaheuristic algorithm, the GWO. It has not been evaluated in the optimization of mineral prospectivity models yet, and this paper tries to address this challenge. Herein, the authors introduce and apply hybrid fuzzy-GWO to a set of independent predictor variables derived from geo-chemical, geological, and structural databases of the Alut area, situated in a significant gold-bearing zone in northwestern Iran for generating efficient gold prospectivity models. So the main goal of this research work is the detection of the gold potential area based on the mineral prospecting mapping by a combination of geo-chemical, geological, and structural information, and then optimization of the detected potential area. The novelty of this research work is the use of GWO in the optimization of the detected area in addition to MPM for the studied area.

2. Case Study

2.1. Tectonic setting and geology

Alut region lies within the northwestern part of the Sanandaj-Sirjan Zone (SSZ), an area covering the Easting coordinate from $45^{0}30'$ to $46^{0}00'$ and Northing coordinates from $36^{0}00'$ to $36^{0}30'$. The Cimmerian elongate sandwich crustal SSZ was separated from Gondwana during the late Paleozoic and started joining Eurasia in the Late Triassic [35, 36].

The SSZ also is considered a margin of Mesozoic subduction between Neo-ethys and Eurasia [37-45]. Calc-alkaline magmatism, regardless of having a relation with arcs [46-48] or belonging to extension and continental rifting [49, 50], is generally estimated to age Middle to Late Jurassic, and is younger in the northern part of SSZ [38]. These plutonics are special properties of SSZ, and occurred as the replacement of the Neoproterozoic to the Paleozoic of crustal basement [47].

Up-drifting of SSZ was caused as a consequence of the Eocene-Early Oligocene collision between Africa-Arabia and Iranian continental blocks [46], and the diagonal closing of the Neotethys [38, 39, 52-55]. Among the tectonic units of Zagros Orogen, the SSZ is the only one that has endured high temperatures of metamorphism. Metamorphic rocks in SSZ include of meta-carbonates, schists, gneisses, and amphibolites [56]. Phanerozoic sediments possessing passive continental margin tolerated some gabbroic to granitic Mesozoic plutons covering them [57].

Due to the intense tectonic activity in the Alut area, numerous overthrusts and displacements with a Northwest-southeast trend parallel to the Zagros fold belt are observed. The common structural trend is N140W, and the primary structural system falls in the shear-overthrust category. This area features the replacement of substantial igneous intrusions, especially in the eastern part of the area that seem to have occurred in a shear-pressure regime. The composition of these intrusions varies from granite to diorite-gabbro with upper Cretaceous age, which has endured some metamorphism to the extent that mylonite fabrics are detectable. Sandstone units in the area have harsh morphology, and are usually developed on high elevations [37, 58, 59].

Folds are the other structure in the Alut region that have less extent under the effect of fault's overcoming. Reverse folds inclined toward the northeast on both sides have limited extension, and are formed in the same-single direction. The valleys eroded by the river's path depend on tectonic situations and fault performance. Such streams' emergence is controlled by the rock's composition besides the dip and direction of structural units [37, 60].

The Doran Granit is believed to be the first magmatic phase in the area that has intruded into Precambrian metamorphic rocks. The oldest geological units are metamorphic rocks including Schist, phyllites, slate, meta rhyolite, and genesis. The degree of metamorphism among these units is considered medium to low. Metamorphic rocks have a direction similar to Zagros overthrust (Northwest-southeast) with a soft morphology. High-latitude Cretaceous units, which encompass sedimentary-volcanic rocks lacking Triassic and

Jurassic ones, have outcrops in the area. Among the boundaries between the Paleozoic and Cretaceous ages, the Permian limestones exist but do not have considerable roots and particular stratigraphic order. Color mélange assemblage occurred in a continental rift southwest of the area during the Paleocene age [61, 62] (Figure 1).

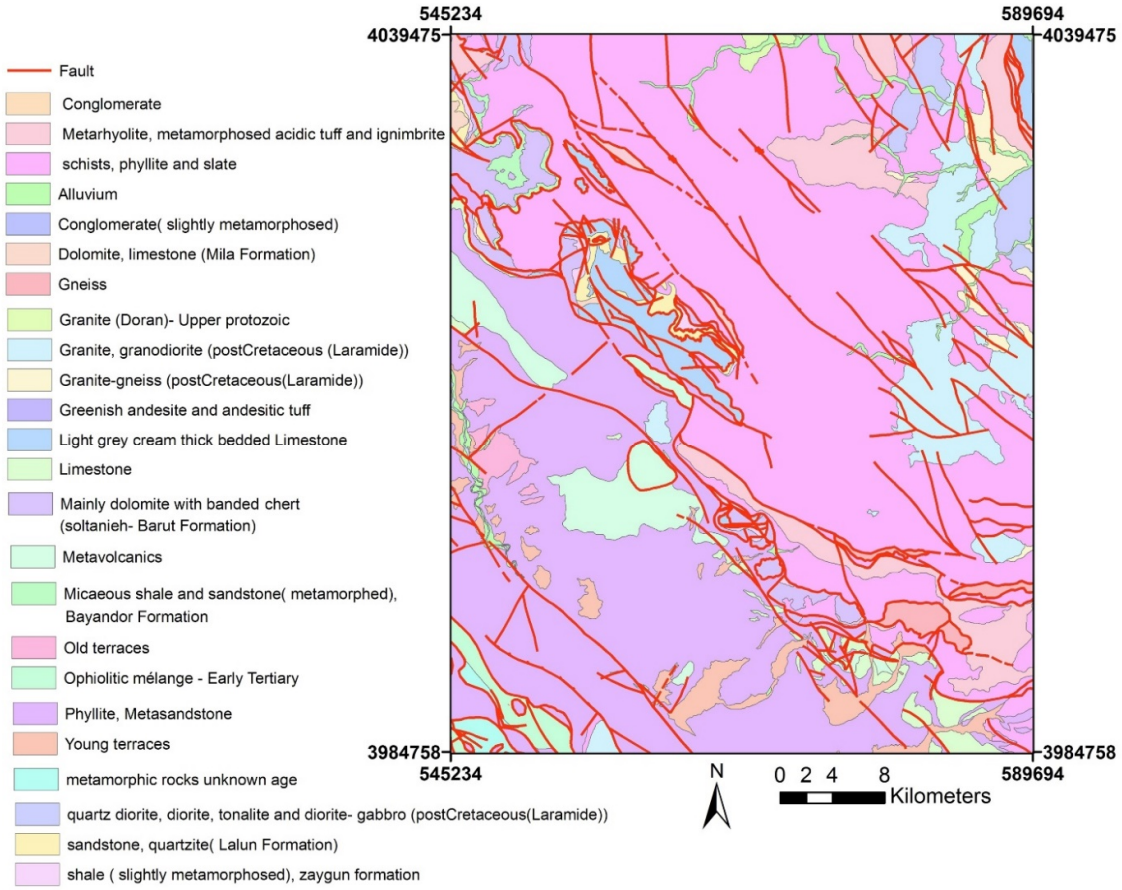

Figure 1. Geology map of the studied area [37].

2.2. Gold mineralization

Most large gold deposits in Iran have been explored within the Sanandaj-Sirjan Zone (SSZ). This belt hosts orogenic, epithermal, porphyry, carlin, and VMS gold mineralization, and is divided into three episodes- early Miocene (16-24Ma), middle Miocene (10-12Ma), and late Miocene (> 8Ma)-, in which the gold mineralization occurs within first two episodes [62, 63]. Structural and geo-chemical features of such mineralization systems have been the subject of numerous studies [32, 33, 57, 59], and used for this study. Although there are some deposits in this zone that are attributed to short-term volcanic activity (i.e. disruption in an extensional tectonic regime beside an association with magma production and injection) like Muteh and Astaneh, however, a significant number of deposits belong to the gold orogenic category. The age of gold mineralization among orogenic gold deposits claimed to be Late Cretaceous to Tertiary, confirming the intense metamorphism during regional Cretaceous-Paleocene convergence and compression. Mineralization mechanism in deposits like Qolqoleh, Kervian, Qabaqloujeh, Kharapeh, and Zartorosht indicates a compressional phase coincidence with Late Cretaceous to Early-Middle Tertiary [32, 64-72].

There are two types of gold mineralization in this area: a) gold mineralization related to shear zones such as Zavakoh, Mirgenakhshineh, and Sheikh Choopan and b) gold mineralization related to gold-rich massive sulfides with volcanic host rock, for example, Barika [60, 62]. A schematic illustration of gold mineralization within the Orogenic system has been displayed in Figure 2. Faults (thrusts) play a principal role in the formation of such deposits and act as leading clues for mineral explorers. According to studies on gold

orogenic mineralization in SZZ [57-61], the most important and abundant hydrothermal alteration accompanied with mineralization consists of argillic and propylitic. Also, they mentioned the main gold-related ore as pyrite, chalcopyrite, and arsenopyrite.

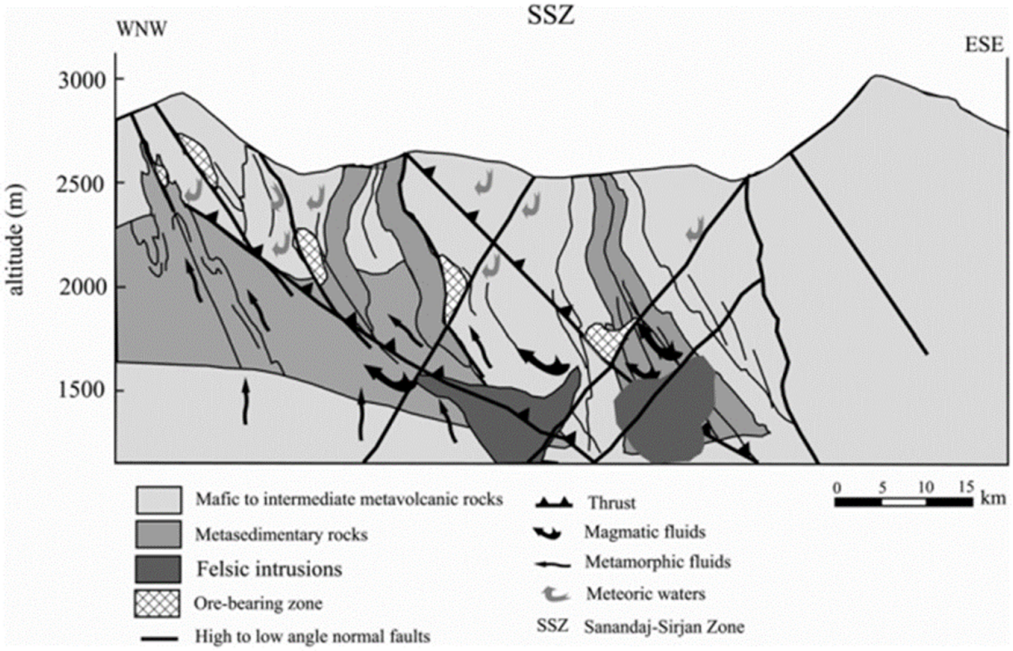

Figure 2. Schematic Orogenic gold mineralization within Sanandaj-Sirjan Zone (SSZ) [61].

2.3. Data used

The Alut 1:100,000 geological map, remote sensing, and geo-chemical data were considered as the input data for this study. The faults distribution map within the studied area was delineated by digitizing the original map prepared by [37]. Aster images, which are free-access through the databank of USGS (Earthexplorer.usgs.gov), were selected as the remote sensing data. These images include three bands in the visible and near-infrared parts, six bands in the shortwave infrared part, and five bands in the thermal infrared part, possessing spatial, resolution of 15 m, 30 m, and 90 m, respectively [73]. Mid-infrared and thermal regions have special properties to detect geological resources and areas related to epithermal and hydrothermal alterations [74-76] and have been performed in many cases: [77, 78]. The Aster data related to the Alut area endured geometric and atmospheric corrections, and then were applied to distinguish argillic and propylitic alteration zones within the Alut area.

The geo-chemical data over the Alut area belong to a sediment geochemical survey with 835 samples and a density of one sample per 3 km^2. The collected samples were sieved by 200 mesh screens in the field, and analyzed with the Inductively Coupled Plasma Mass Spectrometry (ICP-MS) for twenty major elements including Au, As, and Sb.

According to statistical analysis and fractal methods [79] applied to derived sediment stream data, the Au is considered to be paragneiss with Sb, As, Hg, and Mo. While the grade distribution map for Hg and Mo delineates the boundaries of gold mineralization, common areas between Au, As, and Sb would be favorable targets for exploration studies.

3. Methods

3.1. Exploration criteria

The mineral system approach provides a general understanding of geological interactions contributing to ore formation through different geological settings including technical, physical, and chemical processes [1, 3, 76]. These processes are categorized [3, 32, 81-83] as (i) stimulating mineral occurrence with production of required energy gradient; (ii) extraction of agents responsible for ore formation including metals, fluids, and ligands, mantel or crustal origins; (iii) transportation of ore-forming components between source and depositional spots within pathway like faults; (iv) alteration and decomposition of metalliferous fluid caused by physical and

chemical processes occurred within depositional spots leading to ore formation; (v) production or deposits. Unlike the descriptive and genetic models, the mineral system approach considers the ore mineralization with a broader spatial and time frame [3, 84], leading to act as a proper method to uncover new mineral potential at large scales.

The orogenic gold deposits have a close affinity with regionally metamorphosed terranes belonging to different ages. Ore formations occurred through compressional to transgressional deformation interaction within convergent plate margins in both accretionary and collisional regimes. Regardless of orogenic type, hydrated marine sedimentary and volcanic rocks have been intruded into continental margins during long geological time. Thermal events caused by subduction increase the geothermal gradient, and make an easy for fluid to circulate within rocks and produce mineralized and altered zones [85]. Due to covering vast terrains of the Alut area with metamorphosed rocks, it does not seem helpful to specify an evidence layer to lithology, and instead, another factor like faults should be highlighted. Ore-bearing fluids in orogenic systems can replace a considerable volume of gold from high pressure and temperature conditions, i.e. 5 Kbar and 6000C to the surficial properties, i.e. 1 Kbar and 2000C [86]; such transportations happen through the faults networks, and getting distance from them leads to a less chance of mineralization.

Metal precipitation through hydrothermal systems originates from abrupt modifications in physical and chemical properties of fluids that weaken the metal solubility, and involve fluid cooling, depressurization, fluid mixing, and reaction between fluid and rock [3, 10, 80]. Geo-chemical anomalies and hydrothermal alterations are considered conclusive guidance for the detection of chemical deposition. Au, As, and Sb anomalies derived from stream sediment data interpretation beside argillic and propylitic alteration resulting from Aster images were applied as gold mineralization indicators for this study.

3.2. Exploration targeting score approach

There have been various strategies to integrate the evidence layer aiming to make a knowledge-based model. To avoid the subjectivity accompanied by geologists assigning weights to ore formation contributing factors (source, transport, and deposition criteria), it is recommended to apply a set of stochastically simulated weights [87]. Monte Carlo Simulation (MCS), as a solution to respond to this need, has been applied to generate such set weights to model evidence layers [88, 90]. A linear summation of contributing factors that have been weighted by the measures derived from MCS, is defined as desired exploration targeting score approach.

3.3. GWO algorithm

GWO is inspired by the defined social level and behavior of wolves when they decide to hunt animals. Wolves live as a pack and have four social classifications including alpha (α), beta (β), delta (∂), and Omega (ώ) [22].

3.3.1. Social levels

The social life of wolves has been displayed in Figure 3. Accordingly, at the highest point of this pyramid, alpha wolves behave as leaders of the pack and are responsible for making daily decisions. In the second place, beta wolves obey from alpha's orders and thoughts, deltas are ready to receive their duty from the upper classes and finally, omegas are controlled by three other major groups, and contribute to making balance in the social structure.

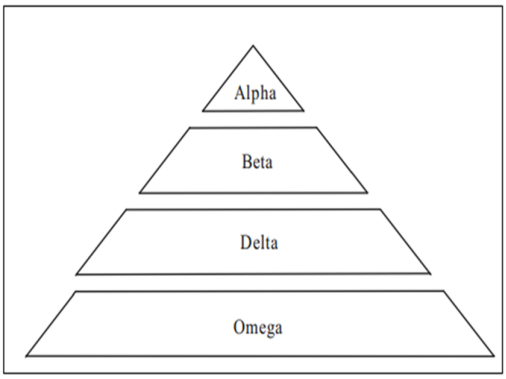

Figure 3. Social hierarchy classification of gray wolf [85].

3.3.2. Hunting process

Gray wolves gain an interesting strategy to make a successful effort while chasing their prey. It is composed of three main steps: decreasing the distance as possible from the prey, compelling the prey to stop moving, and attacking.

In GWO, the best solution belongs to alpha wolf, and the below equations have been introduced by [85]:

$$D = \left|C.x_p(t) - x(t)\right| \quad (1)\ [91]$$

$$x_{(t+1)} = x_p(t) - A.D \quad (2)\ [92]$$

where t refers to irritation number; x_p presents the location of prey; and x is the location of a gray wolf; and C and A applied to create two searching coefficient vectors:

$$A = 2a.r_1 - a \quad (3)\ [92]$$

$$C = 2r_2 \quad (4)\ [92]$$

where a is linearly reduced in [0, 2], and r_1 and r_2 involve random vectors with a measure of [0, 1].

In this algorithm, the prey is considered the best solution, and the alpha has maximum merit to follow the prey. Omegas modified their location with the help of the other three main groups led to finding the best solution. The following equation has been proposed by [22] to explain the process of updating the location:

$$D_\alpha = |C_1 x_\alpha(t) - x(t)| \quad (5)\ [91]$$

$$D_\beta = \left|C_2 x_\beta(t) - x(t)\right| \quad (6)\ [91]$$

$$D_\partial = |C_3 x_\partial(t) - x(t)| \quad (7)\ [91]$$

where $C_i = 2 * r_{i1}$, r_{i1} is a random vector in [0, 1], and $i = 1.2.3$

$$X_1 = |X_\alpha(t) - A_1.D_\alpha| \quad (8)\ [91]$$

$$X_2 = \left|X_\beta(t) - A_2.D_\beta\right| \quad (9)\ [91]$$

$$X_3 = |X_\partial(t) - A_3.D_\partial| \quad (10)\ [92]$$

$$X = {(X_1 + X_2 + X_3)}/{3} \quad (11)\ [92]$$

where:

$$A_i = 2a.r_{i2} - a$$

where r_{i2} involves a random vector in [0, 1] and $X_\alpha(t)$, $X_\beta(t)$, and $X_\partial(t)$ imply the position of alpha, beta, and delta at the t irritation [91].

4. Results

According to the explanation presented in the Section "3.1. Exploration criteria" and due to the objective goal of this study (i.e. prediction of high potential zones of orogenic gold mineralization in the Alut area), the fault systems, Au, As, and Sb anomalies, and Argillic and Propylitic alterations were used to for MPM.

4.1. Knowledge-driven model

To make an efficient knowledge-driven model, according to contributing factors including Au, As, and Sb grade distribution beside the distances from faults, argillic, and propylitic alterations, the exploration targeting score approach applied by [87] was performed. This method calculates the summation of derived fuzzed values for each raster location and considers that as the mean value raster or exploring targeting, the score of each cell. Then these obtained exploration targeting scores are used to make a risk analysis. In this regard, the raster values of each factor were transformed into values between 0.001 and 0.99 based on the relation defined by [94, 95] for positive and negative criteria. Figure 4 displays these fuzzy rasters accompanied by the location of six explored mineral indices within the Alut geological sheet.

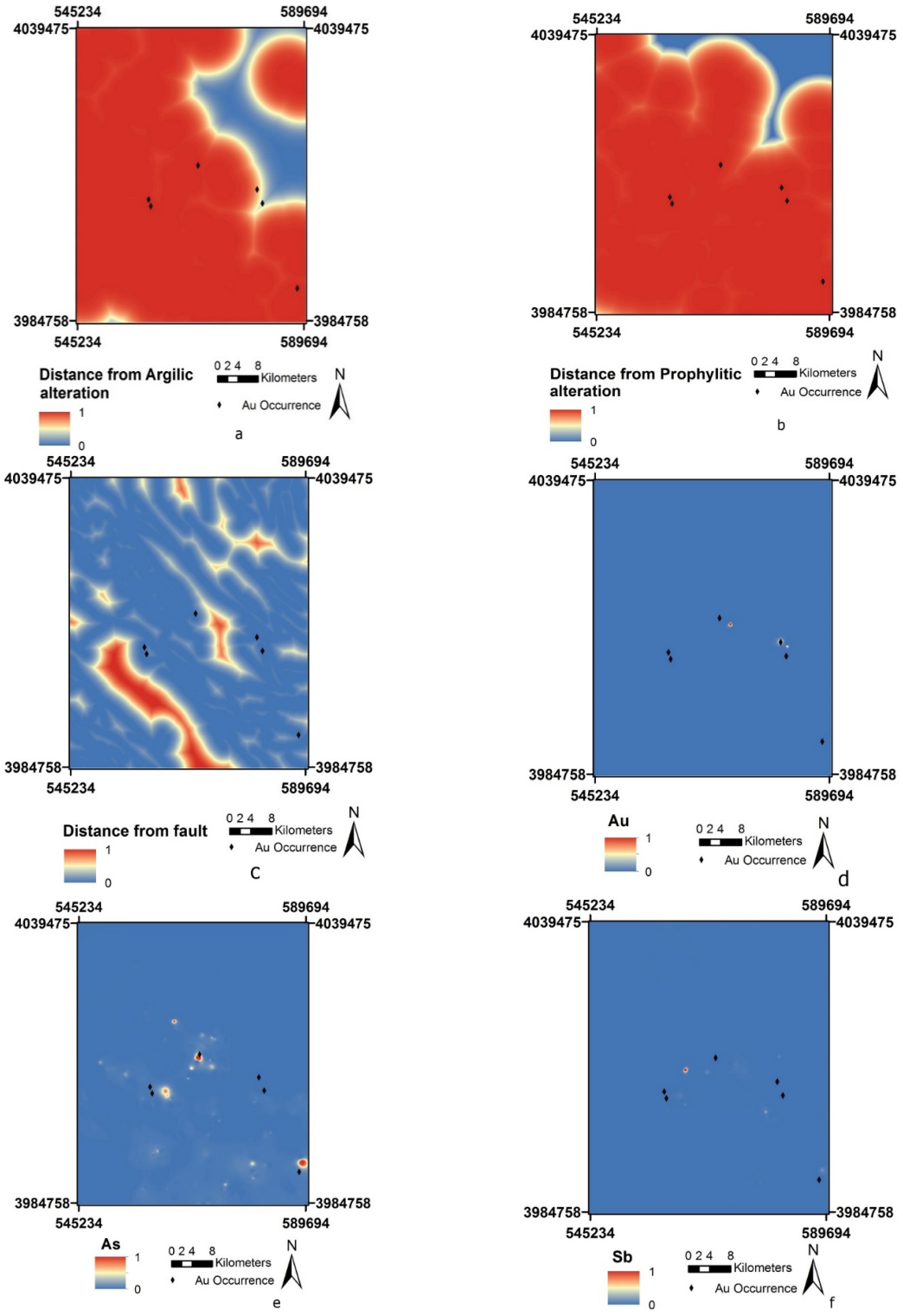

Figure 4. Fuzzified raster maps of mineral system-derived exploration targeting criteria: a) distance from argillic alteration, b) distance from propylitic alteration, c) distance from main faults, d) Au grade distribution, e) As grade distribution, f) Sb grade distribution.

Through the Monte Carlo simulation as a proper method to produce criteria weights, a normal distribution with the mean and standard deviation of 0.5 and 0.2 were selected, and the simulation process continued for 100 iterations. Considering the derived weights and converting them into relative weights, they were prepared for building models. Accordingly, one hundred models were made by a linear sum of criteria in each raster location for every weight set value. The derived mean and standard deviation raster has been illustrated in Figure 5.

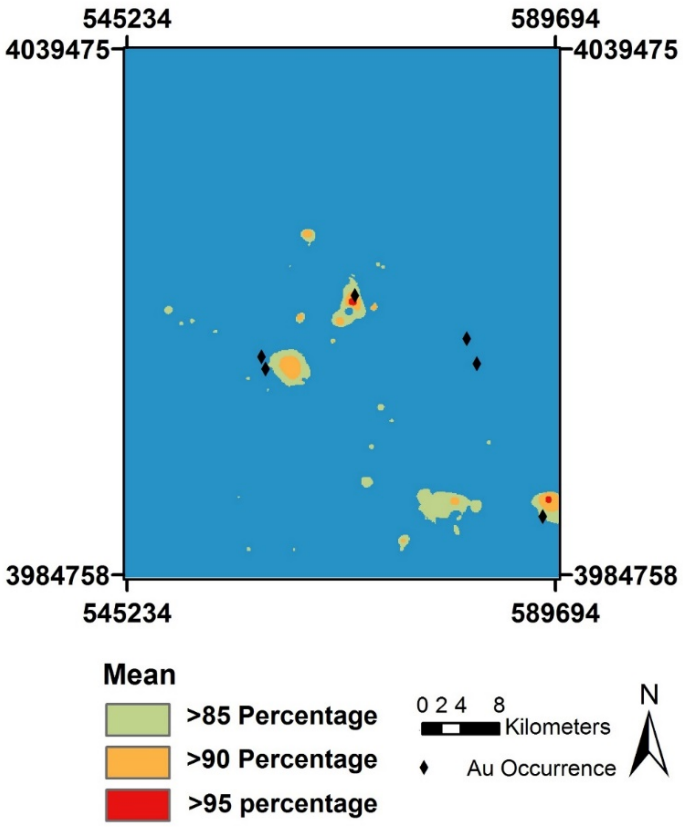

Figure 5. Raster result of derived modeling mean raster.

Besides the mentioned method and results, we here introduce a novel framework that consists of applying GWO on the mean raster model and deriving the optimized value. In other words, zones having greater optimized value should be considered as desired locations.

4.2. Optimization of mean model by GWO

Although the average prospectivity map provides a primary interpretation of zones with high potential for gold mineralization, it includes a spectrum that varies between 0.189 and 0.789. So it is required that this model endures optimization. There are numerous algorithms that are applied to reach this goal. In this study, we used the GWO to optimize the mean map. A gray wolf algorithm with a maximum iteration of 100 and a pack including 50 wolves was designed, in which the following function was considered as the cost function:

$$f(x) = \sum_{i=1}^{n} |x - x_i| \quad (12)$$

where x is the desired optimized value, i $refers$ to the mean raster value at the i[th] previous-explored deposit, and n is the number of Au occurrences within the studied area. The optimized x is where Equation 12 possesses minimum value. While running the algorithm, the function evaluation was investigated 5000 times.

The algorithm has been able to act properly since it reached the optimized solution through the initial iterations, as it has been displayed in Figure 6.

The result of running this code led to the revealing of the optimized cost value of 0.28425,

which belongs to 0.575 among mean raster values. This mean value is equal to 64% of the mean range. In other words, areas that possess higher mean values than 64% of their mean range fall within optimized locations. Figure 7 displays the optimized region derived by applying the GWO.

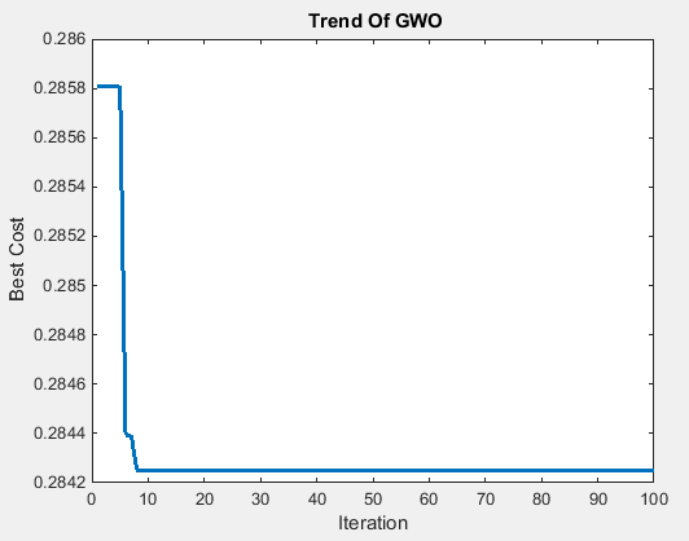

Figure 6. Trend result of gray wolf optimizer (GWO) on mean raster.

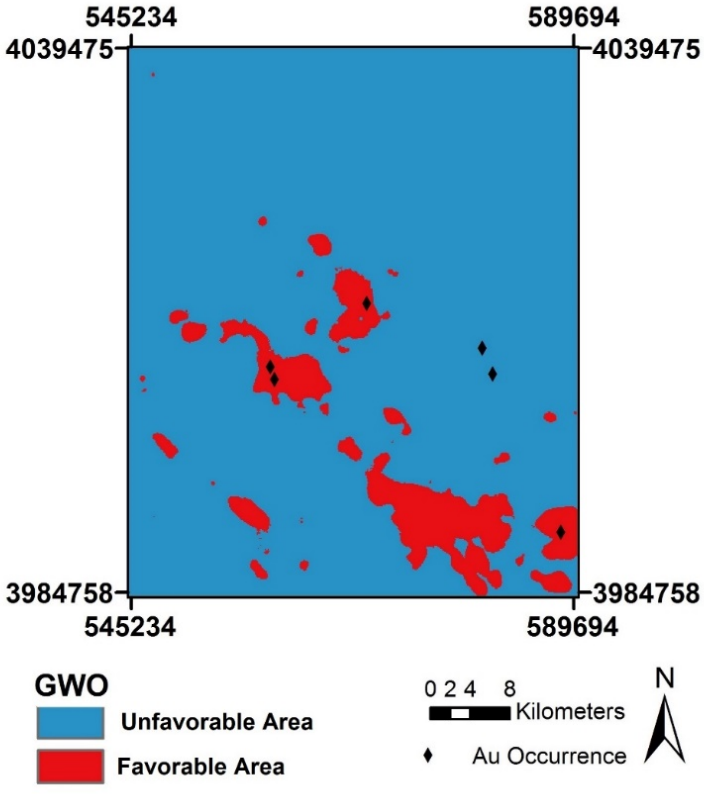

Figure 7. Raster map of the optimized area by GWO within the Alut sheet.

5. Discussion

MPM has a main role in mineral exploration, so various research for MPM has been done and is done. There are different models in MPM for target detection by statistical methods, neural networks, fuzzy methods, hybrid methods, etc. These methods have advantages and disadvantages according to their theory. One of the common and widely used methods in MPM and geo-chemical studies is preparing classified maps based on percentile values.

As mentioned, the main goal of this research work is optimization in the detection of the target area for mineral prospectivity mapping. So the required raster maps were prepared and fuzzies (Figure 4). In next, we prepared the MPM model maps based on the percentile value for 85%, 90%, and 95% presented in Figure 5. According to the prepared MPM map (Figure 5), with the increases of the threshold, the area detected as the exploratory target decreases. The certainty increases with the increase of the threshold limit, but the mineralization areas may be determined outside the exploratory priority. In this study, about 33% of the known gold occurrences were identified with this method.

To achieve better results, we used the GWO. This algorithm is an optimization algorithm; we used it for the first time in mineral prospecting mapping. Based on the GWO, optimization in the final raster map for MPM was done (Figure 7), and the obtained results were compared. The prosperity of our optimization could be evaluated through two approaches:

Firstly, the model's ability to involve explored gold occurrence within the proposed areas. By the GWO, we detected about 66% of explored gold occurrence in the study area, while 33% of known Au occurrence was detected by percentile maps.

Secondly, the extent of optimum areas to the areas introduced by other methods like mean percentiles.

Considering the derived result, an optimized raster involves more gold mineralization occurrence. In addition, the GWO raster covers more area than the percentile methodology. If we consider the limitations of the derived-by-percentile methodology, it is possible to miss some potential areas.

6. Conclusions

We used the gray wolf optimizer (GWO) algorithm, which is an optimization algorithm and a data-driven method, to target detection in the mineral prospecting mapping (MPM) of the Alut area.

By using this algorithm, the interference of the expert's opinion is removed, and the decision to select the target is based on the output of the algorithm, so human errors are minimized.

In the Alut area, as it was expected, the raster map of MPM derived by applying GWO covers more surface of area that eliminates the risk of losing possible mineralization and includes more number of previously explored gold mineralization occurrences as well (66% by GWO versus 33% by percentile).

This study proves that using metaheuristic algorithms should be considered as a proper method to find appropriate search space for exploration activity. The biggest advantage of this novel framework is the independency of statistical uncertainty theories.

As a novel work and opening a new window to MPM knowledge, this study established a new framework that could be elaborated and refined in future studies.

References

[1]. Carranza, E. J. M. (2008). Geochemical anomaly and mineral prospectivity mapping in GIS. Elsevier.

[2]. Afzal, P., Yousefi, M., Mirzaie, M., Ghadiri-Sufi, E., Ghasemzadeh, S., and Daneshvar Saein, L. (2019). Delineation of podiform-type chromite mineralization using geochemical mineralization prospectivity index and staged factor analysis in Balvard area (SE Iran). *Journal of Mining and Environment, 10*(3), 705-715.

[3]. Yousefi, M., Kreuzer, O. P., Nykänen, V., and Hronsky, J. M. (2019). Exploration information systems–A proposal for the future use of GIS in mineral exploration targeting. *Ore Geology Reviews, 111*, 103005.

[4]. Abedi, M., Kashani, S. B. M., Norouzi, G. H., and Yousefi, M. (2017). A deposit scale mineral prospectivity analysis: A comparison of various knowledge-driven approaches for porphyry copper targeting in Seridune, Iran. *Journal of African Earth Sciences, 128*, 127-146.

[5]. Seyedrahimi-Niaraq, M. and Mahdiyanfar, H. (2021). Introducing a new approach of geochemical anomaly intensity index (GAII) for increasing the probability of exploration of shear zone gold mineralization. *Geochemistry, 81*(4), 125830.

[6]. Yousefi, M., Carranza, E. J. M., Kreuzer, O. P., Nykänen, V., Hronsky, J. M., and Mihalasky, M. J. (2021). Data analysis methods for prospectivity modeling as applied to mineral exploration targeting: State-of-the-art and outlook. *Journal of Geochemical Exploration, 229*, 106839.

[7]. Ghasemzadeh, S., Maghsoudi, A., Yousefi, M., and Mihalasky, M. J. (2022). Information value-based geochemical anomaly modeling: A statistical index to generate enhanced geochemical signatures for mineral exploration targeting. *Applied Geochemistry, 136*, 105177.

[8]. Rahimi, H., Abedi, M., Yousefi, M., Bahroudi, A., and Elyasi, G. R. (2021). Supervised mineral exploration targeting and the challenges with the selection of deposit and non-deposit sites thereof. *Applied Geochemistry, 128*, 104940.

[9]. Afzal, P., Farhadi, S., Boveiri Konari, M., Shamseddin Meigooni, M., and Daneshvar Saein, L. (2022). Geochemical anomaly detection in the Irankuh District using Hybrid Machine learning technique and fractal modeling., *Geopersia, 12*(1), 191-199.

[10]. Yousefi, M. and Hronsky, J. M. (2023). Translation of the function of hydrothermal mineralization-related focused fluid flux into a mappable exploration criterion for mineral exploration targeting. *Applied Geochemistry, 149*, 105561.

[11]. Ghaeminejad, H., Abedi, M., Afzal, P., Zaynali, F., and Yousefi, M. (2020). A fractal-based outranking approach for integrating geochemical, geological, and geophysical data. *Bollettino Di Geofisica Teorica Ed Applicata, 61*(4), 555-588.

[12]. Yousefi, M., Barak, S., Salimi, A., and Yousefi, S. (2023). Should Geochemical Indicators Be Integrated to Produce Enhanced Signatures of Mineral Deposits? A Discussion with Regard to Exploration Scale. *Journal of Mining and Environment, 14*(3), 1011-1018. doi: 10.22044/jme.2023.13160.2398.

[13]. Mohammadpour, M., Abedi, M., and Bahroudi, A. (2020). Mineral prospectivity mapping of porphyry Cu deposit using VIKOR method, *Earth Observation and Geomatics Engineering, 4*(2), 148-168.

[14]. Afzal, P., Yasrebi, A. B., Saein, L. D., and Panahi, S. (2017). Prospecting of Ni mineralization based on geochemical exploration in Iran. *Journal of Geochemical Exploration, 181*, 294-304.

[15]. Mokhtari, A. R., Rodsari, P. R., Fatehi, M., Shahrestani, S., and Pournik, P. (2014). Geochemical prospecting for Cu mineralization in an arid terrain-central Iran. *Journal of African Earth Sciences, 100*, 278-288.

[16]. Mahdiyanfar, H. and Seyedrahimi-Niaraq, M. (2022). Improvement of geochemical prospectivity mapping using power spectrum–area fractal modeling of the multi-element mineralization factor (SAF-MF). *Geochemistry: Exploration, Environment, Analysis, 22*(4), geochem2022-015.

[17]. Farhadi, S., Afzal, P., Boveiri Konari, M., Daneshvar Saein, L., and Sadeghi, B. (2022). Combination of Machine Learning Algorithms with Concentration-Area Fractal Method for Soil Geochemical Anomaly Detection in Sediment-Hosted Irankuh Pb-Zn Deposit, Central Iran, *Minerals, 12*(6), 689.

[18]. Seyedrahimi-Niaraq, M., Mahdiyanfar, H., and Mokhtari, A. R. (2023). Application of geochemical structural methods to determine lead-contaminated areas related to mining activities. *Journal of Analytical and Numerical Methods in Mining Engineering, 13*(34), 41-55.

[19]. Barak, S., Imamalipour, A., and Abedi, M. (2023). Application of Fuzzy Gamma Operator for Mineral Prospectivity Mapping, Case Study: Sonajil Area. *Journal of Mining and Environment, 14*(3), 981-997. doi: 10.22044/jme.2023.12954.2352.

[20]. Derrac, J., García, S. and Molina, D. (2011). A practical tutorial on the use of non-parametric statistical tests as a methodology for comparing evolutionary and swarm intelligence algorithms. *Journal of Swarm and Evolutionary Computation. 1*, 3–18.

[21]. Cui, Z. H. and Gao, X. Z. (2012). Theory and applications of swarm intelligence. *Journal of Neural Computing and Applications*. *21*, 205–206.

[22]. Faris, H., Aljarah, I., Al-Betar, M. A., and Mirjalili, S. (2018). Grey wolf optimizer: a review of recent variants and applications. *Neural computing and applications, 30*, 413-435.

[23] Parpinelli, R. S. and Lopes, H. S. (2011). New inspirations in swarm intelligence: a survey. *Journal of International Journal of Bio-Inspired Computation*, *3,* 1–16.

[24] Leboucher, C., Chelouah, R., Siarry, P., and Le Ménec, S. (2012). A swarm intelligence method combined to evolutionary game theory applied to the resource's allocation problem. *International Journal of Swarm Intelligence Research (IJSIR)*, *3*(2), 20-38.

[25]. Zhang, Z., Long, K., Wang, J., and Dressler, F. (2013). On swarm intelligence inspired self-organized networking: its bionic mechanisms, designing principles and optimization approaches. *IEEE Communications Surveys & Tutorials*, *16*(1), 513-537.

[26]. Sulaiman, M. H., Mustaffa, Z., Mohamed, M. R., and Aliman, O. (2015). Using the gray wolf optimizer for solving optimal reactive power dispatch problem. *Applied Soft Computing*, *32*, 286-292.

[27]. Li, S. Y., Wang, S. M., Wang, P. F., Su, X. L., Zhang, X. S., and Dong, Z. H. (2018). An improved grey wolf optimizer algorithm for the inversion of geoelectrical data. *Acta Geophysica*, *66*(4), 607-621.

[28]. Nadimi-Shahraki, M. H., Taghian, S., and Mirjalili, S. (2021). An improved grey wolf optimizer for solving engineering problems. *Expert Systems with Applications*, 166, 113917.

[29]. Afzal, P., Ghasempour, R., Mokhtari, A. R., and Haroni, H. A. (2015). Application of concentration-

number and concentration-volume fractal models to recognize mineralized zones in North Anomaly iron ore deposit, Central Iran. *Archives of Mining Sciences, 60*(3).

[30]. Mahdiyanfar, H. and Seyedrahimi-Niaraq, M. (2023). Integration of Fractal and Multivariate Principal Component Models for Separating Pb-Zn Mineral Contaminated Areas. *Journal of Mining and Environment, 14*(3), 1019-1035.

[31]. Tolouei, K., Moosavi, E., Tabrizi, A. H. B., Afzal, P., and Bazzazi, A. A. (2020). Improving the performance of open-pit mine production scheduling problem under grade uncertainty by hybrid algorithms. *J. Cent. South Univ, 27*, 2479-2493.

[32]. Almasi, A., Yousefi, M., and Carranza, E. J. M. (2017). Prospectivity analysis of orogenic gold deposits in Saqez-Sardasht Goldfield, Zagros Orogen, Iran. *Ore Geology Reviews, 91*, 1066-1080.

[33]. Yousefi, M., Yousefi, S., and Kamkar Rouhani, A. G. (2023). Recognition coefficient of spatial geological features, an approach to facilitate criteria weighting for mineral exploration targeting. *International Journal of Mining and Geo-Engineering, 57-3*,251-258.

[34]. Nykänen, V., Niiranen, T., Molnár, F., Lahti, I., Korhonen, K., Cook, N., and Skyttä, P. (2017). Optimizing a knowledge-driven prospectivity model for gold deposits within Peräpohja Belt, Northern Finland. *Natural Resources Research, 26*(4), 571-584.

[35]. Ricou, L.E. (1974). Letude geologiqes de la region de neyriz (Zagros Iraniaen) et levolution structuraldes zagride. These Universite, Paris, 300.

[36]. Stampfli, G. M. and Borel, G. D. (2004). The TRANSMED transects in space and time: constraints on the paleotectonic evolution of the Mediterranean domain. In The TRANSMED Atlas. The Mediterranean region from crust to mantle (pp. 53-80). Springer, Berlin, Heidelberg.

[37]. Omrani, J. and Khabaznia, A, R. (2003). Geological map of Alut, Scale: 1000000, Geological survey and mineral Exploration of Iran.

[38]. Agard, P., Omrani, J., Jolivet, L., and Mouthereau, F. (2005). Convergence history across Zagros (Iran): constraints from collisional and earlier deformation. *International journal of earth sciences*, *94*(3), 401-419.

[39]. Agard, P., Omrani, J., Jolivet, L., Whitechurch, H., Vrielynck, B., Spakman, W., and Wortel, R. (2011). Zagros orogeny: a subduction-dominated process. *Geological Magazine*, *148*(5-6), 692-725.

[40]. Alavi, M. (1980). Tectonostratigraphic evolution of the Zagrosides of Iran. *Geology*, *8*(3), 144-149.

[41]. Berberian, M. and King, G. C. P. (1981). Towards a paleogeography and tectonic evolution of Iran. *Canadian journal of earth sciences*, *18*(2), 210-265.

[42]. Gansser, Augusto (1981). The geodynamic history of the Himalaya. *Zagros Hindu Kush Himalaya Geodynamic Evolution 3*: 111-121.

[43]. Mohajjel, M., Fergusson, C. L., and Sahandi, M. R. (2003). Cretaceous–Tertiary convergence and continental collision, Sanandaj–Sirjan zone, western Iran. *Journal of Asian Earth Sciences*, *21*(4), 397-412.

[44]. Mohajjel, M. and Fergusson, C. L. (2014). Jurassic to Cenozoic tectonics of the Zagros Orogen in northwestern Iran. *International Geology Review*, *56*(3), 263-287.

[45]. Stampfli, G. M. and Kozur, H. W. (2006). Europe from the Variscan to the Alpine cycles. Memoirs-*Geological Society of London, 32*, 57.

[46]. Berberian, Manuel (1981). Active faulting and tectonics of Iran. *Zagros Hindu Kush Himalaya Geodynamic Evolution 3*: 33-69.

[47]. Hassanzadeh, J. and Wernicke, B. P. (2016). The Neotethyan Sanandaj-Sirjan zone of Iran as an archetype for passive margin-arc transitions. *Tectonics*, *35*(3), 586-621.

[48]. Shahbazi, H., Siebel, W., Pourmoafee, M., Ghorbani, M., Sepahi, A. A., Shang, C. K., and Abedini, M. V. (2010). Geochemistry and U–Pb zircon geochronology of the Alvand plutonic complex in Sanandaj–Sirjan Zone (Iran): New evidence for Jurassic magmatism. *Journal of Asian Earth Sciences*, *39*(6), 668-683.

[49]. Azizi, H. and Stern, R. J. (2019). Jurassic igneous rocks of the central Sanandaj–Sirjan zone (Iran) mark a propagating continental rift, not a magmatic arc. *Terra Nova, 31*(5), 415-423.

[50]. Hunziker, D., Burg, J. P., Bouilhol, P., and von Quadt, A. (2015). Jurassic rifting at the Eurasian Tethys margin: Geochemical and geochronological constraints from granitoids of North Makran, southeastern Iran. *Tectonics*, *34*(3), 571-593.

[51]. Morley, C. K., Kongwung, B., Julapour, A. A., Abdolghafourian, M., Hajian, M., Waples, D., and Kazemi, H. (2009). Structural development of a major late Cenozoic basin and transpressional belt in central Iran: The Central Basin in the Qom-Saveh area. *Geosphere*, *5*(4), 325-362.

[52]. Francois, T., Agard, P., Bernet, M., Meyer, B., Chung, S. L., Zarrinkoub, M. H., and Monie, P. (2014). Cenozoic exhumation of the internal Zagros: first constraints from low-temperature thermochronology and implications for the build-up of the Iranian plateau. *Lithos*, *206*, 100-112.

[53]. Mulch, A., Uba, C. E., Strecker, M. R., Schoenberg, R., and Chamberlain, C. P. (2010). Late Miocene climate variability and surface elevation in the central Andes. *Earth and Planetary Science Letters*, *290*(1-2), 173-182.

[54]. Şengör, A. M. C., Altıner, D., Cin, A., Ustaömer, T., and Hsü, K. J. (1988). Origin and assembly of the Tethyside orogenic collage at the expense of Gondwana Land. *Geological Society, London, Special Publications*, *37*(1), 119-181.

[55]. Vincent, S. J., Allen, M. B., Ismail-Zadeh, A. D., Flecker, R., Foland, K. A., and Simmons, M. D. (2005). Insights from the Talysh of Azerbaijan into the Paleogene evolution of the South Caspian region. *Geological Society of America Bulletin*, *117*(11-12), 1513-1533.

[56]. Ghazi, javad mehdipour, and Mohssen Moazzen (2015). Geodynamic evolution of the Sanandaj-Sirjan zone, Zagros orogen, Iran. *Turkish Journal of Earth Sciences 24.5*: 513-528.

[57]. Dilek, Y., Imamverdiyev, N., and Altunkaynak, Ş. (2010). Geochemistry and tectonics of Cenozoic volcanism in the Lesser Caucasus (Azerbaijan) and the peri-Arabian region: collision-induced mantle dynamics and its magmatic fingerprint. *International Geology Review*, *52*(4-6), 536-578.

[58]. Maghsoudi, Abbas "Gold deposits and indices of Iran", book, 2004.

[59]. Hosseini, S. A., Afzal, P., Sadeghi, B., Sharmad, T., Shahrokhi, S. V., and Farhadinejad, T. (2015). Prospection of Au mineralization based on stream sediments and lithogeochemical data using multifractal modeling in Alut 1: 100,000 sheet, NW Iran. *Arabian Journal of Geosciences*, *8*(6), 3867-3879.

[60]. Mohammadpour, M., Abedi, M., Rahimopor, Gh., Jozanikohan, G., and Khalifiani, F. (2019). Geochemical distribution mapping by combining number-size multifractal model and multiple indicator kriging, *Journal of Geochemical Exploration*, *200*, 13-26. https://doi.org/10.1016/j.gexplo.2019.01.018.

[61]. Ahmadi, F. and Mohamadpour, M. (2018). Geochemical studies of stream sediment to determine the shear zone-related gold mineralization (Case study of Alut area in Kurdistan province). *Iranian Journal of Environmental Geology*, *12*(44), 19-35.

[62]. Aliyari, Farhang, Ebrahim Rastad, and Mohammad Mohajjel (2012). Gold Deposits in the Sanandaj–Sirjan Zone: Orogenic Gold Deposits or Intrusion-Related Gold Systems? *Resource Geology 62*.3: 296-315.

[63]. Heidari, S. M., Afzal, P., and Sadeghi, B. (2022). Miocene tectonic-magmatic events and gold/poly-metal mineralizations in the Takab-Delijan belt, NW Iran. *Geochemistry*, 125944.

[64]. Rashidnezhad, O. N., Emami, M. H., Sabzehei, M., Pique, A., Rastad, E., Bellon, H., and Juteau, T. (2002). Metamorphic and magmatic events of the muteh gold mine (Northeast Golpayegan).

[65]. Kouhestani, H. (2005). Geology, mineralogy, geochemistry and fabrics of gold mineralization in Chah-Bagh shear zones at Muteh mining area (southwest of Delijan, Esfahan province): Unpublished MSc thesis, Tehran, Iran, University of Tarbiat Modares, 222 p.

[66]. Moritz, R., Ghazban, F., and Singer, B. S. (2006). Eocene gold ore formation at Muteh, Sanandaj-Sirjan tectonic zone, Western Iran: a result of late-stage extension and exhumation of metamorphic basement rocks within the Zagros Orogen. *Economic geology*, *101*(8), 1497-1524.

[67]. Rastgoo Moghaddam, G. R., Rastad, E., Rashid Nejad Omran, N., and Mohajel, M. O. H. A. M. M. A. D. (2008). Gold Mineralization in Ductile–Brittle and Brittle Shear Zones, Zartorosht Deposits, Sanandaj-Sirjan Zone, Southwest of Sabzevaran. *Scientific Quarterly Journal of Geosciences*, 17(68), 108-129.

[68]. Aliyari, F., Rastad, E., and Zengqian, H. (2007). Orogenic gold mineralization in the Qolqoleh Deposit, Northwestern Iran. *Resource Geology*, *57* (3), 269–282.

[69]. Aliyari, F., Rastad, E., and Chen, Y. (2008). Fluid inclusion characteristics of the Qolqoleh Gold Deposit, Northwestern Iran. 33rd international geological conference Oslo, Norway. Oral presentation, p. 112.

[70]. Aliyari, F., Rastad, E., and Arehart, G. B. (2009). Geology and geochemistry of D-O-C isotope systematics of the Qolqoleh Gold Deposit, Northwestern Iran: implications for ore genesis. *Ore Geology Review*, *36*, 306–314.

[71]. Heidari, M., Rastad, E., Mohajjel, M., and Shamsa, M. J. (2006) Gold mineralization in ductile shear zone of Kervian (southwest of Saqez-Kordestan province), *Geosciences*, *58*, 18–37.

[72]. Niroomand, S., Goldfarb, R. J., Moore, F., Mohajjel, M., and Marsh, E. E. (2011). The Kharapeh orogenic gold deposit: geological, structural, and geochemical controls on epizonal ore formation in West Azerbaijan Province, Northwestern Iran. *Mineralium Deposita*, *46*(4), 409-428.

[73] Abrams, M., Tsu, H., Hulley, G., Iwao, K., Pieri, D., Cudahy, T., and Kargel, J. (2015). The advanced spaceborne thermal emission and reflection radiometer (ASTER) after fifteen years: review of global products. International *Journal of Applied Earth Observation and Geoinformation*, *38*, 292-301.

[74]. Ninomiya, Y. (2003, March). Rock type mapping with indices defined for multispectral thermal infrared ASTER data: case studies. *In Remote Sensing for Environmental Monitoring, GIS Applications, and Geology II* (Vol. 4886, pp. 123-132). SPIE.

[75]. Pour, A. B. and Hashim, M. (2012). The application of ASTER remote sensing data to porphyry copper and epithermal gold deposits. *Ore geology reviews*, *44*, 1-9.

[76]. Testa, F. J., Villanueva, C., Cooke, D. R., and Zhang, L. (2018). Lithological and hydrothermal

alteration mapping of epithermal, porphyry and tourmaline breccia districts in the Argentine Andes using ASTER imagery. *Remote Sensing*, *10*(2), 203.

[77]. Alimohammadi, Masoumeh, Saeed Alirezaei, and Daniel J. Kontak. (2015). Application of ASTER data for exploration of porphyry copper deposits: A case study of Daraloo–Sarmeshk area, southern part of the Kerman copper belt, Iran. *Ore Geology Reviews 70*: 290-304.

[78]. Pour, A. B. and Hashim, M. (2015). Regional geological mapping in tropical environments using landsat TM and SRTM remote sensing data. *ISPRS Annals of the Photogrammetry, Remote Sensing and Spatial Information Sciences*, *2*(2), 93.

[79]. Afzal, P., Ahari, H. D., Omran, N. R., and Aliyari, F.(2013). Delineation of gold mineralized zones using concentration–volume fractal model in Qolqoleh gold deposit, NW Iran. *Ore Geology Reviews*, *55*, 125-133.

[80]. Sun, T., Chen, F., Zhong, L., Liu, W., and Wang, Y. (2019). GIS-based mineral prospectivity mapping using machine learning methods: A case study from Tongling ore district, eastern China. *Ore Geology Reviews*, *109*, 26-49.

[81]. Wyborn, L. A. I., Heinrich, C., and Jaques, A. L. (1994). Australian Proterozoic mineral systems: Essential ingredients and mappable criteria: Australasian Institute of Mining and Metallurgy. In Darwin Conference, Abstract Series (Vol. 5, p. 94).

[82]. Kreuzer, O. P., Etheridge, M. A., Guj, P., McMahon, M. E., and Holden, D. J. (2008). Linking mineral deposit models to quantitative risk analysis and decision-making in exploration. *Economic Geology*, *103*(4), 829-850.

[83]. Joly, A., Porwal, A., and McCuaig, T. C. (2012). Exploration targeting for orogenic gold deposits in the Granites-Tanami Orogen: Mineral system analysis, targeting model and prospectivity analysis. *Ore Geology Reviews*, *48*, 349-383.

[84]. Hagemann, Steffen G., V. A. Lisitsin, and D. L. Huston (2016). Mineral system analysis: Quo vadis. *Ore Geology Reviews, 76*: 504-522.

[85]. Groves, D. I., Goldfarb, R. J., Gebre-Mariam, M., Hagemann, S. G., and Robert, F. (1998). Orogenic gold deposits: a proposed classification in the context of their crustal distribution and relationship to other gold deposit types. *Ore geology reviews*, *13*(1-5), 7-27.

[86]. Li, H., Wang, Q., Yang, L., Dong, C., Weng, W., and Deng, J. (2022). Alteration and mineralization patterns in orogenic gold deposits: Constraints from deposit observation and thermodynamic modeling. *Chemical Geology*, *607*, 121012.

[87]. Hsu, T. H. and Pan, F. F. (2009). Application of Monte Carlo AHP in ranking dental quality attributes. *Expert Systems with Applications*, *36*(2), 2310-2316.

[88]. Pakyuz-Charrier, E., Lindsay, M., Ogarko, V., Giraud, J., and Jessell, M. (2018). Monte Carlo simulation for uncertainty estimation on structural data in implicit 3-D geological modeling, a guide for disturbance distribution selection and parameterization. *Solid Earth*, *9*(2), 385-402.

[89]. Athens, Noah D., and Jef K. Caers (2019). A Monte Carlo-based framework for assessing the value of information and development risk in geothermal exploration. *Applied Energy, 256*: 113932.

[90]. Yousefi, M. and Gholami, R. (2010). Risk management and decision making in economic systems. First Edition, Jahad Daneshgahi press, Amirkabir University of Technology (in Persian).

[91]. Mirjalili, Seyedali, Seyed Mohammad Mirjalili, and Andrew Lewis (2014). Grey wolf optimizer. *Advances in engineering software*, *69*: 46-61.

[92]. Rodrigues, L. R. (2023). A chaotic grey wolf optimizer for constrained optimization problems. *Expert Systems*, *40*(4), e12719.

[93]. Parsa, M. and Pour, A. B. (2021). A simulation-based framework for modulating the effects of subjectivity in greenfield mineral prospectivity mapping with geochemical and geological data. *Journal of Geochemical Exploration*, *229*, 106838.

[94]. Zimmermann, H. J. (1991). Cognitive sciences, decision technology, and fuzzy sets. *Information Sciences*, *57*, 287-295.

[95]. Porwal, A., Carranza, E. J. M., and Hale, M. (2003). Knowledge-driven and data-driven fuzzy models for predictive mineral potential mapping. *Natural Resources Research*, *12*, 1-25.

تعیین اهداف اکتشافی طلا براساس مدلسازی پتانسیل معدنی با استفاده از یک الگوریتم بهینه‌سازی

کامران مصطفائی[1*]، محمدنبی کیانپور[2] و مهیار یوسفی[3]

۱. بخش مهندسی معدن، دانشکده مهندسی،دانشگاه کردستان، ایران
۲. دانشکده مهندسی معدن، دانشگاه صنعتی امیرکبیر، تهران، ایران
۳. دانشکده مهندسی، دانشگاه ملایر، ملایر، ایران

ارسال ۲۰۲۳/۰۸/۱۳، پذیرش ۲۰۲۳/۰۹/۳۰

* نویسنده مسئول مکاتبات: k.mostafaei@uok.ac.ir

چکیده:

مدلسازی پتانسیل‌های معدنی (MPM) یک فرایند چند مرحله‌ای و ترکیبی است که هدف آن تعین اهدف اکتشافی می‌باشد. دانش متخصصان بخش اصلیمطالعات MPM بوده و در چند مرحله مورد نیاز است. اول) تهیه لایه‌های شاهد، در این مرحله شواهد و فرآیند کانی‌سازی با لایه‌های مختلف تحت عنوان لایه‌های شاهد بیان می‌شود، دوم) تعیین وزن به هر لایه جهت تهیه نقشه نهایی، سوم) تفسیر نقشه‌های تهیه شده جهت پیش‌بینی نواحی کانی‌سازی. مورد دوم از اهمیت خاصی برخوردار است زیرا باید وزن هر لایه مشخص شده و براساس همه آنها یک نقشه پتانسیل کانی‌سازی تهیه شود. بنابراین باید یک برنامه جهت طبقه بندی یا اولویت بندی نواحی اکتشافی تهیه شود و بر اساس آن تصمیم‌گیری شود. در این مقاله تلاش شده تا علاوه بر استفاده از الگوها و روش‌های قبلی، یک الگوریتم جدید، که یک الگوریتم بهینه ساز است، تحت عنوان الگوریتم بهینه‌ساز گرگ خاکستری(GWO) جهت استفاده در مدلسازی پتانسیل معدنی معرفی کند. در این مطالعه از الگوریتم گرگ خاکستری و نقشه چندک‌ها (درصد) میانگین شامل ۸۵، ۹۵ و ۹۵٪ میانگین جهت تعین بهترین نواحی اکتشافی استفاده شد. جهت استفاده از این روش‌ها، برگه صدهزار آلوت در شمال غربی ایران به عنوان مطالع موردی انتخاب شد. مقایسه نتایج بدست آمده نشان داد که نقشه تهیه شده براساس الگوریتم گرگ خاکستری، تعداد اندیس و کانسار بیشتری (تقریبا دوبرابر) نسبت به نقشه درصد میانگین آشکارسازی نمود. همچنین نقشه تهیه شده با الگوریتم گرگ خاکستری نواحی بیشتری به عنوان نواحی مستعد کانی‌سازی شناسایی نمود که ممکن است با بقیه روش‌ها شناسایی نشوند.

کلمات کلیدی: مدلسازی پتانسیل‌های معدنی، الگوریتم بهینه ساز گرگ خاکستری، اهداف اکتشافی طلا.